NOMA Aided Interference Management for Full-Duplex Self-Backhauling HetNets

Lei Lei, Eva Lagunas, Symeon Chatzinotas, and Björn Ottersten

***Abstract*— The presence of mutual-coupled interference in full-duplex self-backhauling heterogeneous networks raises challenges and difficulties in practical scenarios. In this letter, we address this issue by developing a two-tier non-orthogonal multiple access (NOMA) scheme together with efficient power control to enable aggressive frequency reuse and alleviate co-channel interference. For the considered multi-tier and multi-cell NOMA scenario, we formulate a power minimization problem, and develop an efficient algorithm with guaranteed convergence to enable optimal power control, such that users' data demand is satisfied and backhauling bottleneck is avoided. Numerical results show the fast convergence of the proposed algorithm, and demonstrate that NOMA is in particular favorable for the high-demand cases in power savings.**

***Index Terms*— Heterogeneous networks, full-duplex, self-backhauling, non-orthogonal multiple access.**

I. Introduction

THE DENSE deployment of small base stations (SBSs) with wireless backhauling on the overlaid macro base stations (MBSs) forms the so-called self-backhauled heterogeneous networks (HetNets). Since the spectrum resource is scarce and expensive, in-band self-backhauling has emerged as an important enabler to balance the costs with scarce frequency resources [1]. In this context, smart duplexing, e.g., full-duplex (FD) operation, and new radio access techniques, e.g., non-orthogonal multiple access (NOMA), are considered to improve the spectral efficiency and ensure certain quality-of-service (QoS). Adopting aggressive frequency reuse, in-band self-backhauling, and FD techniques in HetNets, introduces four types of interference, i.e., cross-tier, inter-cell, intra-cell interference, and self-interference (see Fig. 1).

Recent progress on FD has enabled suppressing self-interference to satisfactory levels [2]. Extensive studies have been devoted to resource allocation [3] and performance analysis of outage probability [4] in FD single-cell NOMA. Lei *et al.* [5] have studied an FD-NOMA-based relaying systems with one MBS and one SBS. In [6], an FD-based massive MIMO system for both downlink and uplink has been investigated. For multi-cell FD NOMA, Elbamby *et al.* [7] consider utility maximization, and illustrate the performance gains of FD over half-duplex modes. Rate maximization has been widely studied for FD NOMA systems. Due to the presence of strong interference in multi-cell networks, power control is also important. Without a proper solution for interference suppression and power control, achieving higher throughput either in MBS or in SBS links would lead to significant increase in power consumption.

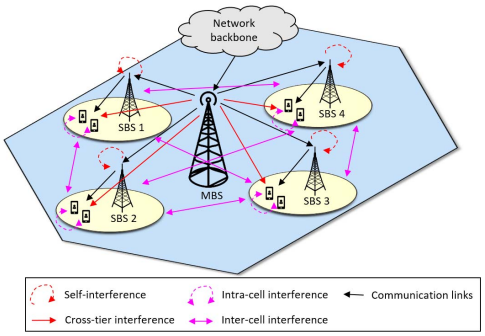

Fig. 1. HetNet scenario with one MBS and four SBSs.

In this letter, our contribution lies in addressing two emerging research issues: (1) how much power-saving gains can be expected by using NOMA in the considered FD in-band self-backhauling HetNets, and (2) how to perform effective and efficient interference management such that all the QoS requirements can be satisfied. Firstly, we propose a two-tier NOMA scheme in the system model, in order to facilitate efficient frequency reuse while alleviating the resulting co-channel interference. Secondly, we derive an optimal solution of jointly determining the decoding order in NOMA and the transmit power. The optimization decisions of power and ordering are intertwined and dependent with each other. In solution development, we characterize the dependence and the properties of the optimization variables. Based on the derived proof, we develop an efficient solution to systematically update decoding order and transmit power, which finally leads to an optimal solution with guaranteed convergence. Numerical results verify the competitiveness of using the proposed two-tier NOMA in high-demand cases, and the convergence of the proposed power control algorithm.

II. System Model

We consider a two-tier self-backhauled HetNet consisting of a single MBS serving S SBSs. All the SBSs are wirelessly connected to the backbone network through the MBS. User equipments' (UEs) traffic is routed through the SBSs nearby. With in-band self-backhauling, all the SBSs and the MBS share the same frequency. All the SBSs operate at the FD mode. Downlink data transmission, i.e., MBS-to-SBSs and SBS-to-UEs, is considered. The basic notations are shown in Table I. The power constraints are stated as follows $P_m = \sum_{s=1}^{S} p_{ms}$ and $P_s = \sum_{k=1}^{|\mathcal{K}_s|} p_{sk}$, $\forall s \in \{1, \ldots, S\}$,

Manuscript received March 1, 2018; revised June 5, 2018; accepted June 6, 2018. Date of publication June 15, 2018; date of current version August 10, 2018. This work has been supported by the FNR CORE project ROSETTA (C17/IS/11632107). The associate editor coordinating the review of this letter and approving it for publication was M. Vaezi. *(Corresponding author: Lei Lei.)*

The authors are with the Interdisciplinary Center for Security Reliability and Trust, University of Luxembourg, L-1855 Luxembourg City, Luxembourg (e-mail: lei.lei@uni.lu; eva.lagunas@uni.lu; symeon.chatzinotas@uni.lu; bjorn.ottersten@uni.lu).

Digital Object Identifier 10.1109/LCOMM.2018.2847672

TABLE I
BASIC NOTATIONS

P_m, P_s	transmit power at the MBS and the s-th SBS
p_{ms}	transmit power from the MBS to the s-th SBS
p_{sk}	transmit power from the s-th SBS to UE k
h_{ms}	channel coefficient from the MBS to the s-th SBS
h_{sk}	channel coefficient from the s-th SBS to UE k
$\hat{h}_{mk}$	channel coefficient from the MBS to UE k
$\hat{h}_{ss'}$	channel coefficient from the s-th SBS to the s'-th SBS
h_{ss}	channel coefficient of self-interference at the s-th SBS
σ_s^2, σ_k^2	noise power at the s-th SBS and at UE k

where $\mathcal{K}_s$ is the set containing all the UEs in the s-th SBS. The received interfering signal at each SBS is determined by the inter-cell interference received from other SBSs, the residual self-interference and the interference received from the MBS transmission intended to other SBSs. We denote $0 \leq \beta_s \leq 1$ to reflect the s-th SBS capability in suppressing its own self-interference [1]–[5]. When $\beta_s = 1$, no self-interference cancellation is made, while $\beta_s = 0$ models perfect self-interference cancellation. The residual self-interference at the s-th SBS's receiver is proportional to the transmit power [1]–[5], defined as $\beta_s \sum_{k=1}^{|\mathcal{K}_s|} p_{sk}$.

To reduce co-channel interference, we apply NOMA in the MBS-to-SBSs transmission, referred to as "first-tier NOMA". The MBS transmits superposed signals to SBSs, and each SBS has the capability of performing successive interference cancellation (SIC). The SIC decoding order among SBSs is defined as the descending order of $\frac{h_{m1}}{I_1}, \ldots, \frac{h_{ms}}{I_s}, \ldots, \frac{h_{mS}}{I_S}$ [5], [7], where $I_s = h_{ss}\beta_s \sum_{k=1}^{|\mathcal{K}_s|} p_{sk} + \sum_{\hat{s}\in\mathcal{S}\setminus\{s\}} P_{\hat{s}}\hat{h}_{\hat{s}s} + \sigma_s^2$. Suppose two SBSs $s = 1, 2$ have $\frac{h_{m1}}{I_1} \geq \frac{h_{m2}}{I_2}$. We assume SBS 2's receiver is able to decode its desired signal x_2. According to the NOMA basis, SBS 1 at its receiver can decode this signal x_2 only if $\frac{P_{m2}h_{m1}}{p_{m1}h_{m1}+h_{11}\beta_1\ P_1+P_2\hat{h}_{21}+\sigma_1^2} \geq \frac{P_{m2}h_{m2}}{p_{m1}h_{m2}+h_{22}\beta_2\ P_2+P_1\hat{h}_{12}+\sigma_2^2}$, where the former is the SINR of signal x_2 at SBS 1's receiver, and the latter represents the SINR of signal x_2 at SBS 2's receiver. One can observe that the inequality holds when $\frac{h_{m1}}{I_1} \geq \frac{h_{m2}}{I_2}$, where $I_1 = h_{11}\beta_1\ P_1 + P_2\hat{h}_{21} + \sigma_1^2$ and $I_2 = h_{22}\beta_2\ P_2 + P_1\hat{h}_{12} + \sigma_2^2$. As a result, SBS 1 can decode and remove part of the interference, with the rate $\log(1+\frac{P_{m1}h_{m1}}{h_{11}\beta_1\ P_1+P_2\hat{h}_{21}+\sigma_1^2})$. SBS 2 will not be able to perform SIC, achieving the rate $\log(1+\frac{P_{m2}h_{m2}}{p_{m1}h_{m2}+h_{22}\beta_2\ P_2+P_1\hat{h}_{12}+\sigma_2^2})$. Applying the first-tier NOMA, the signal-to-interference-plus-noise ratio (SINR) at the s-th SBS can be modeled as SINR_s^{m}. The rate of the MBS towards the s-th SBS is $R_s = \log(1+\text{SINR}_s^{\text{m}})$, where the bandwidth is normalized as 1, with assuming $\frac{h_{m1}}{I_1} \geq, \ldots, \frac{h_{ms}}{I_s}, \ldots, \geq \frac{h_{mS}}{I_S}$.

$$\text{SINR}_s^{\text{m}} = \frac{p_{ms}h_{ms}}{h_{ss}\beta_s\sum\limits_{k=1}^{|\mathcal{K}_s|} p_{sk} + \sum\limits_{\hat{s}=1}^{s-1} p_{m\hat{s}}h_{ms} + \sum\limits_{\hat{s}\in\mathcal{S}\setminus\{s\}} P_{\hat{s}}\hat{h}_{\hat{s}s} + \sigma_s^2}, \quad \forall s \in \mathcal{S}$$

At the transmission of SBS-to-UEs, we introduce "second-tier NOMA" to further mitigate the interference experienced by the UEs. Once the superposed signal from the MBS arrives at each SBS, the SBS decodes and forwards this signal to its associated UEs. At the UEs' side, SIC is applied. Similar to the first-tier NOMA, we sort $\frac{h_{s1}}{I_1^s}, \ldots, \frac{h_{sk}}{I_k^s}, \ldots, \frac{h_{s|\mathcal{K}_s|}}{I_{|\mathcal{K}_s|}^s}$ by the descending order in the s-th SBS, where $I_k^s = P_m\hat{h}_{mk} + \sum_{\hat{s}\in\mathcal{S}\setminus\{s\}} P_{\hat{s}}h_{\hat{s}k} + \sigma_k^2,\ \forall k \in \mathcal{K}_s$. Suppose $\frac{h_{s1}}{I_1^s} \geq, \ldots, \frac{h_{sk}}{I_k^s}, \ldots, \geq \frac{h_{s|\mathcal{K}_s|}}{I_{|\mathcal{K}_s|}^s}$, the SINR of the k-th UE in SBS s is shown in SINR_k^{s}. The k-th UE receives the cross-tier interference $P_m\hat{h}_{mk}$ from the MBS, the intra-cell interference $\sum_{\hat{k}=1}^{k-1} p_{s\hat{k}}h_{sk}$ from the 1-st to the $k-1$-th UEs, as well as the inter-SBS interference $\sum_{\hat{s}\in\mathcal{S}\setminus\{s\}} P_{\hat{s}}h_{\hat{s}k}$. The k-th UE's rate in SBS s is $R_k^s = \log(1+\text{SINR}_k^{\text{s}})$, $k \in \mathcal{K}_s$.

$$\text{SINR}_k^{\text{s}} = \frac{p_{sk}h_{sk}}{\sum\limits_{\hat{k}=1}^{k-1} p_{s\hat{k}}h_{sk} + P_m\hat{h}_{mk} + \sum\limits_{\hat{s}\in\mathcal{S}\setminus\{s\}} P_{\hat{s}}h_{\hat{s}k} + \sigma_k^2}, \quad \forall k \in \mathcal{K}_s$$

III. PROBLEM FORMULATION AND PROPERTY ANALYSIS

The addressed two-tier NOMA aided interference management problem contains two components, i.e., determining optimal decoding orders and power allocation. We aim at minimizing the total transmit power over all the BSs in the objective (1a), such that all the UEs' data requests can be satisfied in (1b). In (1c), since the UEs' traffic is routed through the associated SBS, and the SBS has to request the data to the backbone network through the MBS. To avoid the MBS-SBS link becoming a bottleneck, the data rate of the backhauling link is required to be no less than the aggregated rate of the UE access links. To simplify our presentation, we formulate the power control problem under one of the decoding orders, assuming $\frac{h_{m1}}{I_1} \geq, \ldots, \geq \frac{h_{mS}}{I_S}$, and $\frac{h_{s1}}{I_1^s} \geq, \ldots, \geq \frac{h_{s|\mathcal{K}_s|}}{I_{|\mathcal{K}_s|}^s},\ \forall s \in \mathcal{S}$ for the moment. The joint optimization of decoding order and power control will be addressed later.

$$\textbf{P1}: \min_{P_m,\ P_s,\ p_{ms},\ p_{sk}} \quad P_m + \sum_{s\in\mathcal{S}} P_s \tag{1a}$$

$$\text{s.t. } \log(1+\text{SINR}_k^{\text{s}}) \geq D_k, \quad \forall s \in \mathcal{S},\ \forall k \in \mathcal{K}_s \tag{1b}$$

$$\sum_{k\in\mathcal{K}_s} \log(1+\text{SINR}_k^{\text{s}}) \leq \log(1+\text{SINR}_s^{\text{m}}), \quad \forall s \in \mathcal{S} \tag{1c}$$

$$P_m = \sum_{s=1}^{S} p_{ms}, \quad \text{and } P_s = \sum_{k\in\mathcal{K}_s} p_{sk}, \quad \forall s \in \mathcal{S} \tag{1d}$$

The difficulty lies in jointly determining the optimal decoding order and power allocation. These two components mutually influence with each other. The decoding orders in two-tier NOMA vary with transmit power, and the SINR functions in (1b) and (1c) also depend on the decoding orders. Without knowing optimal power, the optimal decoding order is undetermined, and vice versa. Clearly, traversing all the permutations of decoding orders and solving the corresponding problem (**P1**) under every order, has exponential complexity, and thus inefficient in practice. To solve the joint optimization problem, in Proposition 1 we illustrate how the power $P_m, P_1, \ldots, P_S$ related to each other. We introduce a power vector $\bar{\boldsymbol{p}}_s = [P_m, P_1, \ldots, P_{s-1}, P_{s+1}, \ldots, P_S]$ collecting all the transmit power except the s-th SBS's power P_s.

Proposition 1: P_s submits to a closed-form expression of $\bar{\boldsymbol{p}}_s$.

Proof: For each UE $k \in \mathcal{K}_s$ in the s-th SBS, based on $R_k^s = \log(1+\text{SINR}_k^{\text{s}})$, we can derive each power variable $p_{s1}, \ldots, p_{sk}, \ldots, p_{s|\mathcal{K}_s|}$ in the following equations. Suppose

$\frac{h_{s1}}{I_1^s} \geq, \ldots, \geq \frac{h_{s|\mathcal{K}_s|}}{I^s_{|\mathcal{K}_s|}}$, the decoding order is consistent with the user index in SBS s.

$$p_{s1} = (e^{R_1^s}-1)(P_m\hat{h}_{m1}+\sum_{\hat{s}\in\mathcal{S}\setminus\{s\}} P_{\hat{s}}h_{\hat{s}1}+\sigma_1^2)/h_{s1}=(e^{R_1^s}-1)\frac{I_1^s}{h_{s1}}$$
$$\ldots$$
$$p_{s|\mathcal{K}_s|} = (e^{R^s_{|\mathcal{K}_s|}}-1)(\sum_{\hat{k}=1}^{|\mathcal{K}_s|-1} p_{s\hat{k}}h_{s|\mathcal{K}_s|} + I^s_{|\mathcal{K}_s|})/h_{s|\mathcal{K}_s|}$$

From the above, all the p_{s1} appeared in $p_{s2}, \ldots, p_{s|\mathcal{K}_s|}$ can be replaced by $(e^{R_1^s}-1)\frac{I_1^s}{h_{s1}}$. Next, each p_{s2} existed in $p_{s3}, \ldots, p_{s|\mathcal{K}_s|}$ can be substituted by $(e^{R_2^s}-1)((e^{R_1^s}-1)\frac{I_1^s}{h_{s1}}h_{s2}+I_2^s)/h_{s2}$, and so on, until substituting $p_{s,|\mathcal{K}_s|-1}$ in $p_{s|\mathcal{K}_s|}$. Once this substituting process is complete, we are able to explicitly express $P_s = p_{s1}+, \ldots, +p_{s|\mathcal{K}_s|}$ in (2) by the function of $P_m, P_1, \ldots, P_{s-1}, P_{s+1}, \ldots, P_S$, hence the conclusion.

$$\begin{aligned}
P_s &= -\frac{P_m\hat{h}_{m|\mathcal{K}_s|}+\sum_{\hat{s}\in\mathcal{S}\setminus\{s\}} P_{\hat{s}}h_{\hat{s}|\mathcal{K}_s|}+\sigma^2_{|\mathcal{K}_s|}}{h_{s|\mathcal{K}_s|}} + \sum_{k=1}^{|\mathcal{K}_s|}[e^{\sum_{\hat{k}=k}^{|\mathcal{K}_s|}R^s_{\hat{k}}} \\
&\quad \times(\frac{P_m\hat{h}_{mk}+\sum_{\hat{s}\in\mathcal{S}\setminus\{s\}}P_{\hat{s}}h_{\hat{s}k}+\sigma_k^2}{h_{sk}} \\
&\quad -\frac{P_m\hat{h}_{m,k-1}+\sum_{\hat{s}\in\mathcal{S}\setminus\{s\}}P_{\hat{s}}h_{\hat{s},k-1}+\sigma_{k-1}^2}{h_{s,k-1}})] \\
&= \sum_{k=1}^{|\mathcal{K}_s|}(\frac{I_k^s}{h_{sk}}-\frac{I_{k-1}^s}{h_{s,k-1}})e^{\sum_{\hat{k}=k}^{|\mathcal{K}_s|}R_{\hat{k}}^s} - \frac{I^s_{|\mathcal{K}_s|}}{h_{s|\mathcal{K}_s|}} \\
&= f(P_m, P_1, \ldots, P_{s-1}, P_{s+1}, \ldots, P_S) \qquad (2)
\end{aligned}$$

■

In Proposition 1, we reveal the dependence between P_s and $[P_m, P_1, \ldots, P_{s-1}, P_{s+1}, \ldots, P_S]$. Next, we characterize the function $P_s = f(\bar{\boldsymbol{p}}_s)$ by introducing the concept of standard interference function (SIF). By definition, if a function $f(\boldsymbol{x})$: $\mathbb{R}_+^n \to \mathbb{R}_+^n$, for all the input $\boldsymbol{x}$, satisfies the following three properties: positivity, $f(\boldsymbol{x}) > 0$; monotonicity, if $\boldsymbol{x}' \geq \boldsymbol{x}$ then $f(\boldsymbol{x}') \geq f(\boldsymbol{x})$; and scalability, $\alpha f(\boldsymbol{x}) > f(\alpha\boldsymbol{x})$ for all $\alpha > 1$, then $f(\boldsymbol{x})$ is SIF. Starting from any initial point and performing fixed-point iteration based algorithm, the convergence of the proposed method is guaranteed [8].

Proposition 2: $f(\bar{\boldsymbol{p}}_s),\ \forall s \in \mathcal{S}$, *is SIF.*

Proof: From the proof of Proposition 1, the positivity can be observed. For monotonicity, we increase all the elements in $\bar{\boldsymbol{p}}_s$ by a positive value $\epsilon > 0$, i.e., $\bar{\boldsymbol{p}}_s' = \bar{\boldsymbol{p}}_s + \epsilon$, and substitute all the entities $P_m, P_1, \ldots, P_{s-1}, P_{s+1}, \ldots, P_S$ in (2) by $P_m + \epsilon$, $P_1 + \epsilon, \ldots, P_{s-1} + \epsilon, P_{s+1} + \epsilon, \ldots, P_S + \epsilon$. As a result, all the values of $p_{s1}, p_{s2}, \ldots, p_{s|\mathcal{K}_s|}$ are strictly increased. Since $P_s = \sum_{k\in\mathcal{K}_s} p_{sk}$ then $f(\bar{\boldsymbol{p}}_s') > f(\bar{\boldsymbol{p}}_s)$. In terms of scalability, let $\alpha > 1$ and derive $\alpha f(\bar{\boldsymbol{p}}_s)$ and $f(\alpha\bar{\boldsymbol{p}}_s)$ as follows,

$$\begin{aligned}
&\alpha f(\bar{\boldsymbol{p}}_s) \\
&= (e^{R_1^s}-1)(\alpha P_m\hat{h}_{m1} + \sum_{\hat{s}\in\mathcal{S}\setminus\{s\}} \alpha P_{\hat{s}}h_{\hat{s}1} + \alpha\sigma_1^2)/h_{s1}+, \ldots, \\
&\quad + \frac{e^{R^s_{|\mathcal{K}_s|}}-1}{h_{s|\mathcal{K}_s|}}(\alpha\sum_{\hat{k}=1}^{|\mathcal{K}_s|-1} p_{s\hat{k}}h_{s|\mathcal{K}_s|} + \alpha P_m\hat{h}_{m|\mathcal{K}_s|} \\
&\quad + \alpha\sum_{\hat{s}\in\mathcal{S}\setminus\{s\}} P_{\hat{s}}h_{\hat{s}|\mathcal{K}_s|} + \alpha\sigma^2_{|\mathcal{K}_s|})
\end{aligned}$$

$$\begin{aligned}
&f(\alpha\bar{\boldsymbol{p}}_s) \\
&= (e^{R_1^s}-1)(\alpha P_m\hat{h}_{m1} + \sum_{\hat{s}\in\mathcal{S}\setminus\{s\}} \alpha P_{\hat{s}}h_{\hat{s}1} + \sigma_1^2)/h_{s1}+, \ldots, \\
&\quad + \frac{e^{R^s_{|\mathcal{K}_s|}}-1}{h_{s|\mathcal{K}_s|}}(\sum_{\hat{k}=1}^{|\mathcal{K}_s|-1} p_{s\hat{k}}h_{s|\mathcal{K}_s|} + \alpha P_m\hat{h}_{m|\mathcal{K}_s|} \\
&\quad + \alpha\sum_{\hat{s}\in\mathcal{S}\setminus\{s\}} P_{\hat{s}}h_{\hat{s}|\mathcal{K}_s|} + \sigma^2_{|\mathcal{K}_s|})
\end{aligned}$$

It can be observed that $\alpha f(\bar{\boldsymbol{p}}_s) > f(\alpha\bar{\boldsymbol{p}}_s)$. Hence the conclusion follows. ■

Analogously to the proof of Proposition 1 and 2, we reach the following similar results for P_m in Corollary 3.

Corollary 3: P_m is a function of $\bar{\boldsymbol{p}}_m$, and $P_m = f(\bar{\boldsymbol{p}}_m)$ is SIF.

Proof: Assuming $\frac{h_{m1}}{I_1} \geq, \ldots, \frac{h_{ms}}{I_s}, \ldots, \geq \frac{h_{mS}}{I_S}$, P_m can be expressed by a closed-form function $f(\bar{\boldsymbol{p}}_m)$ in (3), where $\bar{\boldsymbol{p}}_m = [P_1, \ldots, P_S]$ and $P_m = f(\bar{\boldsymbol{p}}_m)$.

$$P_m = \sum_{s=1}^{S}(\frac{I_s}{h_{ms}} - \frac{I_{s-1}}{h_{m,s-1}})e^{\sum_{\hat{s}=s}^{S}R_{\hat{s}}} - \frac{I_S}{h_{mS}} = f(\bar{\boldsymbol{p}}_m) \qquad (3)$$

The property of SIF follows analogously. ■

Remark 1: The three properties of SIF in $f(\bar{\boldsymbol{p}}_m)$ and $f(\bar{\boldsymbol{p}}_s)$ are independent with the SIC decoding order. Thus, $f(\bar{\boldsymbol{p}}_m)$ and $f(\bar{\boldsymbol{p}}_s)$ are SIF under any of possible decoding orders. □

Algorithm 1 Jointly Determining Decoding Orders and Power Allocation

1: Initialize power vectors $\boldsymbol{p} = [P_m', P_1', \ldots, P_S']$ and $\boldsymbol{p}^* = [P_m, P_1, \ldots, P_S]$
2: $R_k^s \leftarrow D_k, \forall k \in \mathcal{K}_s, \forall s \in \mathcal{S}_k$, $R_s \leftarrow \sum_{k\in\mathcal{K}_s} D_k, \forall s \in \mathcal{S}$
3: **while** $||\boldsymbol{p}^* - \boldsymbol{p}||_2 > \gamma$ **do**
4: $\quad \boldsymbol{p} \leftarrow \boldsymbol{p}^*$
5: $\quad$ Update the decoding order of the first-tier NOMA as the descending order of $\frac{h_{m1}}{I_1}, \ldots, \frac{h_{mS}}{I_S}$
6: $\quad$ Obtain power P_m by (3) with the new decoding order
7: $\quad$ **for** $s = 1 : S$ **do**
8: $\quad\quad$ Update the decoding order of the second-tier NOMA as the descending sequence of $\frac{h_{s1}}{I_1^s}, \ldots, \frac{h_{s|\mathcal{K}_s|}}{I^s_{|\mathcal{K}_s|}}$
9: $\quad\quad$ Obtain power P_s by (2) under the updated order
10: $\quad \boldsymbol{p}^* = [P_m, P_1, \ldots, P_S]$

By our analysis, thus far we are able to develop a fixed-point iteration based algorithm, see Algorithm 1, to jointly optimize the two-tier NOMA decoding orders and the power allocation. That is, we adjust $P_m, P_1, \ldots, P_S$ one by one. When a power variable is updating, all the others remain fixed. Even though the power adjustment in a cell has mutual-influence effect to the other cells, having proven the property of SIF, this procedure will eventually converge to a fixed power point which leads to the optimum [8]. Algorithm 1 terminates when the Euclidean distance between the power vectors of two successive iterations, given by the 2-norm $||\boldsymbol{p}^* - \boldsymbol{p}||_2$, is smaller than a tolerate value $\gamma = 10^{-5}$.

TABLE II
SIMULATION PARAMETERS

Parameter	Value
Cell radius	300 m
Carrier frequency	2 GHz
Bandwidth	1 MHz
Number of UEs	2, 5
Number of MBS and SBSs	1 and 4
Coefficient β_s	0.5
Channel model	ITU urban macro/micro-cell model
Noise power	-173 dBm/Hz

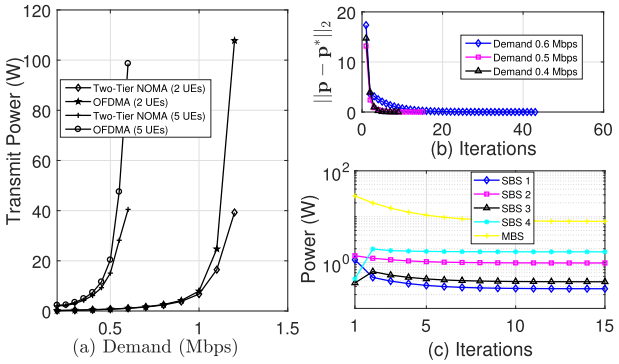

Fig. 2. (a), total power with respect of demand and number of UEs; (b), evolution of convergence in Alg. 1; (c), evolution of power in all the cells.

IV. NUMERICAL RESULTS

We present numerical results to illustrate the performance of the two-tier NOMA scheme and the algorithm, in terms of power savings and convergence. The simulation parameters are summarized in Table II. An optimal power allocation scheme for orthogonal frequency division multiple access (OFDMA) networks, presented in [9], is implemented for comparison. To enable a fair comparison between FD-OFDMA and FD-NOMA, we require that all the cells in [9] are active, and all the SBSs are operating at the FD mode. The revised algorithm provides an optimal power solution for full-duplex based OFDMA HetNets. All the numerical results are averaged over 1000 realizations.

In Fig. 2a and Table III, compared with [9], we show the power-saving gains due to applying NOMA and the proposed Algorithm 1. The two-tier NOMA demonstrated its superiority, evidenced by consistently less power consumption than OFDMA. We observe that the performance gains of NOMA over OFDMA is relatively marginal for the low-demand cases, less than 10%, while for the high-demand instances, NOMA starts to demonstrate its significant gains of power savings which can achieve 1.5-2 times power reduction than OFDMA. This also means that NOMA yields better capability in supporting UEs' increasing demand. In practice, the total power consumption also grows successively with increase of number of UEs and BSs, and the level of residual self-interference [3], [5]. In contrast, power increases exponentially with the UEs' demand, and thus it is considered as a dominant factor in the simulation.

Next, in Fig. 2b, we reveal the evolution of convergence in Algorithm 1. We use the cases of 5 UEs per SBS for illustration. For the three different demands, in average the convergence is reached after around 8, 14, 43 iterations, respectively. When the demand increases, more iterations are required for convergence. In addition, from Table III, the

TABLE III
SUMMARY OF THE PERFORMANCE IN FIG. 2A

Demand (2 UEs):	0.6	0.8	1.0	1.1	1.2
Gaps	4.2%	7.3%	17.7%	50.1%	174.3%
Ava. Iter.	6.2	8.3	11.9	21.3	41.8
Demand (5 UEs):	0.4	0.45	0.5	0.55	0.6
Gaps	19.6%	25.0%	34.9%	68.5%	143.6%
Ava. Iter.	8.2	9.6	14.1	25.4	43.1

number of UEs also influences the required iterations to converge, but the effect appears moderate. In general, Algorithm 1 is capable of converging fast. In Fig. 2c, we illustrate the evolution of transmit power of SBSs and the MBS in the algorithm's execution. The cases of demand $=$ 0.5 Mbps are used. All the cells' transmit power can be successively reduced over iterations until reaching the convergence, although the effect of interference suppression may not necessarily be monotonic. By applying Algorithm 1, the mutual-coupled ICI can be eventually suppressed or maintained at an optimal level without causing performance degradation to the other parts. In the meanwhile, the system consumes the minimum power to satisfy all the constraints in **P1**.

V. CONCLUSION

We have developed an efficient iterative algorithm with guaranteed optimality and convergence for the NOMA aided FD in-band self-backhauling HetNets. The proposed two-tier NOMA scheme and the iterative algorithm are able to significantly reduce the required power consumption than OFDMA in particular for the cases of high demand. A promising extension of the current work is to investigate the potential gains of power control under the imperfections of NOMA, e.g., imperfect channel estimation and SIC, as well as developing efficient distributed algorithms for interference management. Another extension is to incorporate the SIC delay NOMA in FD operation and investigate the time-domain resource scheduling.

REFERENCES

[1] A. Sabharwal *et al.*, "In-band full-duplex wireless: Challenges and opportunities," *IEEE J. Sel. Areas Commun.*, vol. 32, no. 9, pp. 1637–1652, Sep. 2014.
[2] M. S. Sim *et al.*, "Nonlinear self-interference cancellation for full-duplex radios: From link-level and system-level performance perspectives," *IEEE Commun. Mag.*, vol. 55, no. 9, pp. 158–167, Jun. 2017.
[3] Y. Sun *et al.*, "Optimal joint power and subcarrier allocation for full-duplex multicarrier non-orthogonal multiple access systems," *IEEE Trans. Commun.*, vol. 65, no. 3, pp. 1077–1091, Mar. 2017.
[4] Z. Mobini *et al.*, "Full-duplex multi-antenna relay assisted cooperative non-orthogonal multiple access," in *Proc. IEEE GLOBECOM*, Dec. 2017, pp. 1–7.
[5] L. Lei *et al.*, "Energy optimization for full-duplex self-backhauled HetNet with non-orthogonal multiple access," in *Proc. IEEE SPAWC*, Jul. 2017, pp. 1–5.
[6] X. Xia *et al.*, "Beam-domain full-duplex massive MIMO: Realizing co-time co-frequency uplink and downlink transmission in the cellular system," *IEEE Trans. Veh. Technol.*, vol. 66, no. 10, pp. 8845–8862, Oct. 2017.
[7] M. S. Elbamby *et al.*, "Resource optimization and power allocation in in-band full duplex-enabled non-orthogonal multiple access networks," *IEEE J. Sel. Areas Commun.*, vol. 35, no. 12, pp. 2860–2873, Dec. 2017.
[8] R. D. Yates, "A framework for uplink power control in cellular radio systems," *IEEE J. Select. Areas Commun.*, vol. 13, no. 7, pp. 1341–1347, Sep. 1995.
[9] L. Lei *et al.*, "Optimal cell clustering and activation for energy saving in load-coupled wireless networks," *IEEE Trans. Wireless Commun.*, vol. 14, no. 11, pp. 6150–6163, Nov. 2015.